Proceedings of the 5th World Congress on Mechanical, Chemical, and Material Engineering (MCM'19)
Lisbon, Portugal – August, 2019
Paper No. HTFF 141
DOI: 10.11159/htff19.141

Reactive Turbulent Flow Model Of Anode Baking Furnace To Estimate NOx Through Zeldovich Mechanism

Prajakta Nakate[1,2], Domenico Lahaye[1], Cornelis Vuik[1]
[1]Delft University of Technology
Van Mourik Broekmanweg 6, 2628 XE, Delft, Netherlands
P.A.Nakate@tudelft.nl; D.J.P.Lahaye@tudelft.nl; C.Vuik@tudelft.nl
[2]Aluminium & Chemie (Aluchemie) Rotterdam B.V.
Oude Maasweg 80, 3197 KJ, Botlek, Netherlands

Abstract **-** Anode baking process has gained significant attention since the 1980s due to its high contribution to costs. The process involves various physics such as turbulent flow, combustion process, radiation and conjugate heat transfer which are highly dependent on each other. The process needs optimization for reducing NOx, saving energy and achieving a higher quality of anodes. A mathematical model of the anode baking furnace can provide significant information for improving the process. The goal of the present work is to find solutions for reducing NOx formation.

The research method is chosen based on the simple models for each physics so as to have initial results. The complexity of the model is gradually increased. In this paper, a 2D reactive turbulent flow model of the heating section of the furnace is developed for initial analysis. The results are qualitatively analysed and the distribution of velocity, mass fractions of chemical species and temperature are presented. The distribution aligns with the expected physical behaviour of the system. Radiation in participating media is considered by modelling planck mean absorption coefficient. The temperature seems to be affected significantly by radiation. At the post-processing stage, Zeldovich mechanism is applied to calculate the source term for NOx and thereby, a distribution of mole fraction of NOx in the heating section is estimated. The NOx generation is observed in the high-temperature zone of the furnace as would be expected in reality. Furthermore, a 3D non-reactive flow model is developed and the results of velocity are compared with 2D. Analysis of the velocity in the Z direction suggests a significant difference in the velocity field near the fuel inlet. Therefore, for studying the mixing dominated combustion models, a 3D model is essential.

Keywords**:** Turbulent flow, Eddy dissipation model, Combustion, NOx, Zeldovich mechanism.

1. Introduction

Anodes are the major components in the extraction process of Aluminium from bauxite ore in Hall- Hèroult process. The cost of anodes accounts up to 15% and therefore, are considered to be important [1]. The anodes in their raw state contain 85% of dry products and 15% of the pitch [2]. In the baking process of anodes, the pitch is evaporated and anodes with desired properties such as higher mechanical strength and higher conductivity are produced. The anode baking process consists of multiple physical phenomena such as turbulent flow, combustion process, conjugate heat transfer, and radiation. The process needs a vast amount of energy and also releases undesired gases such as CO, CO_2, and NO_x. Therefore, an ideal anode baking process needs an optimization in terms of reduction in NOx, soot-free combustion, reducing energy utilization and improving quality of anodes. This can be achieved by optimization of the process by mathematically modelling the interdependence of multiple physical phenomena.

The mathematical modelling of the anode baking process has been developed and improved significantly in past years. In 1983 Bui. et. al. attempted to simulate horizontal flue ring furnace in which they treated furnace as a counter-flow heat exchanger [3]. Many models that are developed at the later stage are based on these early developed models. A more detailed 3D modelling of the flue of anode baking furnace started in the mid-90s. Kocaefe et. al. presented a model in which a commercial CFD code CFDS-FLOW3D was used for solving the governing differential equations [4]. However, this model used simplified combustion and radiation models failing to comment on the pollutants. Severo and Gusberti developed a user-friendly software to analyse furnace energy efficiency, minimum oxygen concentration in different sections [1]. However, for obtaining more specific data related to soot or NOx formation with higher accuracy, the tool cannot be considered. More recently, a dynamic process model was developed by Oumarou et. al. to investigate the effect of

temperature variation in the vertical component by considering a vertical component of flue gas [2], [5], [6]. This allows the 2D temperature distribution boundary condition for the pit sub model. However, the model fails to optimize reducing emissions, saving energy and maintaining anode quality. Moreover, in the previous work, the eddy dissipation model was used in most of the work for modelling combustion. It is well known that the eddy dissipation model overestimates the temperature. The effect of other combustion models is explored by Grègoire and Gosselin. In their work, a comparison of three combustion models for anode baking furnace is carried out in Ansys Fluent [7]. Similar work is carried out by Tajik. et. al. in which effect of flue wall design on the flow field, combustion and temperature has been modelled in Ansys Fluent [8], [9]. The finite volume method is used in Ansys Fluent. Whereas, COMSOL® Multiphysics is based on the finite element method. It would be interesting to compare the results with two approaches. In conclusion, vast modelling approaches are developed for anode baking furnace. However, the model for NOx reduction still needs significant attention.

The main aim of the present work is to develop a model that provides an estimate of the generation of NOx. In the present paper, a 2D reactive turbulent flow model is developed and a rough distribution of NOx is presented. The results of this model align with the expected physical behaviour of the system. However, the validation with actual data from the furnace is required as a next step of the work. A brief analysis of P1 approximation radiation model with planck mean absorption coefficient suggests the sensitivity of model with respect to radiation. Further improvement in the radiation mechanism is needed in the model. The present model quantifies NOx with the Zeldovich mechanism and shows a mole fraction distribution of NOx. A rough comparison with the actual data proposes that the estimation of NOx generation is highly underestimated. Furthermore, the results of a 3D non-reactive turbulent flow model are presented. The results show a necessity of a 3D model to achieve improvement in combustion modelling which is mixing dominated.

2. Model Equations

An anode baking furnace involves the occurrence of multiple physical phenomena. In order to have a detailed understanding of the process, the complex physics can be expressed in terms of mathematical equations which further can be solved based on certain assumptions. In this section, the well-known models that are used to solve turbulent flow, combustion reaction, radiation and simplified calculations of NOx are explained.

In this model, the complexity of turbulent flow is simplified by considering time averaged Navier-Stokes equation (RANS). The turbulence fluctuation is assumed not to affect density and therefore, incompressible turbulent flow is considered. In order to close the Reynolds stress term, a k-ε model is used. The flow equations used in this model are as shown in Eq. 1 – Eq. 6. All symbols have their standard meaning as mentioned in the list of symbols given in Appendix.

$$\rho \nabla \cdot (u) = 0 \tag{1}$$

$$\rho(u \cdot \nabla)u = \nabla \cdot [-pI + (\mu + \mu_T)(\nabla u + (\nabla u)^T)] \tag{2}$$

$$\rho(u \cdot \nabla)k = \nabla \cdot \left[\left(\mu + \frac{\mu_T}{\sigma_k}\right)\nabla k\right] + P_k - \rho\varepsilon \tag{3}$$

$$\rho(u \cdot \nabla)\varepsilon = \nabla \cdot \left[\left(\mu + \frac{\mu_T}{\sigma_\varepsilon}\right)\nabla k\right] + C_{\varepsilon 1}\frac{\varepsilon}{k}P_k - C_{\varepsilon 2}\rho\frac{\varepsilon^2}{k} \tag{4}$$

$$\mu_T = \rho C_\mu \frac{k^2}{\varepsilon} \tag{5}$$

$$P_k = \mu_T[\nabla u: (\nabla u + (\nabla u)^T)] \tag{6}$$

The eddy dissipation model is used for defining the combustion reaction. The transport equation for each chemical species i, is given by the Eq. 7- Eq. 9. A regularization is used so that the reaction is terminated once the reactant mass fraction approaches zero.

$$\nabla \cdot j_i + \rho(u \cdot \nabla)w_i = R_i \tag{7}$$

$$j_i = -\left(\rho D_i^f \nabla w_i + \rho w_i D_i^f \frac{\nabla M_n}{M_n} - \rho w_i \sum_k \frac{M_i}{M_n} D_k^f \nabla x_k + D_i^T \frac{\nabla T}{T}\right) \tag{8}$$

$$R_i = \upsilon_i M_i \frac{\alpha}{\tau_T} \min\left[min\left(\frac{w_r}{\upsilon_r M_r}\right), \beta \sum_p \frac{w_p}{\upsilon_p M_p}\right] \tag{9}$$

The process involves transport of heat by the gas streams as well as the generation of heat due to the combustion reaction. Therefore, the heat transport equation as shown in Eq. 10 is also of importance. Heat source term (q_0) in Eq. 10 is defined in terms of heat of reaction and extent of reaction. The P1 approximation model is used for simplifying radiation in the process. The equations governing P1 approximation model are given by Eq. 11 and Eq. 13.

$$d_z \rho C_p u \cdot \nabla T + \nabla \cdot (-d_z k_T \nabla T) = q_0 + d_z Q_r \tag{10}$$

$$Q_r = \kappa(G - 4\pi I_b) \tag{11}$$

$$\nabla \cdot (D_{P1} \nabla G) + \kappa(G - 4\pi I_b) = 0 \tag{12}$$

$$D_{P1} = \frac{1}{3(\kappa + \sigma_s)} \tag{13}$$

Lastly, for calculation of NOx distribution at the post-processing stage, a Zeldovich mechanism equation (Eq. 14) is used for computing a source term of convection-diffusion equation of NOx (Eq. 15). For calculating O radical concentration, equilibrium assumption is used. Also, as the mixture is lean, the OH concentration is assumed to be negligible. Moreover, it should be noted that the concentration of NO from Eq. 14 can be replaced in terms of mole fraction of NO in order to substitute it in Eq. 15. Here, S_{NO} is the source term for NOx.

$$S_{NO} = M_{NO} \frac{d[NO]}{dt} = M_{NO}\left[2k_f[O][N_2] \frac{\left(1 - \frac{k_{r,1}k_{r,2}[NO]^2}{k_{f,1}[N_2]k_{f,2}[O_2]}\right)}{\left(1 + \frac{k_{r,1}[NO]}{k_{f,2}[O_2]}\right)}\right] \tag{14}$$

$$\nabla \cdot (-D_i \nabla x_{NO}) + u \cdot \nabla x_{NO} = S_{NO} \quad (15)$$

The boundary conditions for solving these equations are elaborated in the next section on simulation details.

3. Simulation Details

The modelling of the anode baking process presented in this paper is carried out in COMSOL® Multiphysics software. This software is based on finite element method and provides a powerful platform for modelling of multiple physics. The research method is chosen such that the complexity of the model is gradually increased by adding physics. The choice of models for different physics is based on the ease of implementation. However, considering the accuracy requirement for the current practical application the choice of these models can be justified.

The mesh for the model is prepared by inspecting wall resolution of few trial models, as the convergence behaviour is highly affected by the elements at the corners and boundaries. This is due to the high gradients at boundaries. Wall functions are used as boundary conditions for the wall. The air and fuel velocity in 2D is adjusted such that it mimics the actual air/fuel ratio in the furnace. Five chemical species namely, CH_4, O_2, CO_2, H_2O and N_2 with a single step reaction of CH_4 with O_2 is considered in the model. The eddy dissipation model defines the turbulence-chemistry interaction in this model. Therefore, the turbulence time scale used in the reaction source term is calculated by coupling turbulent flow equations with that of transport equations of chemical species. The specific heat capacities of all the chemical species are calculated by a piecewise cubic interpolation function and by using the available thermodynamic data from literature. The temperature at the inlet is specified based on the available average temperature data from Aluchemie furnace in different sections. The analysis of the absorption radiation parameter is carried out assuming an emissivity of surfaces to be 0.6. The assumption is based on the emissivity data provided by the supplier of refractory bricks. Inlet and Outlet boundaries are assumed to be black surfaces. Boundary conditions for NOx equation are based on the assumption that the inlet streams do not contain any traces of NOx. The natural gas that is used in the furnaces is recorded to have low NOx amount. The diffusion of NOx in a direction parallel to the outlet boundary is defined to be zero. The total concentration in the model is calculated based on the density and mean molar mass of the mixture.

The model is assumed to be at steady state. As the fire cycle time is as long as 48 hours for one cycle, the steady state assumption is reasonable. The model uses the Newton-Raphson method to solve nonlinear equations. A segregated solver with different damping coefficients for different variables is used for better convergence. Moreover, at each Newton iteration, the accuracy of each step is adjusted. The MUMPs direct solver is used for 2D models whereas, the FGMRES iterative solver with a domain decomposition preconditioner is used for 3D models.

4. Results and Discussion

In this section, the results that are obtained during the numerical simulation of the heating section of the anode baking furnace are discussed. The section is divided into two subsections based on the dimensions of the model. In the first subsection results of the 2D reactive turbulent flow model are presented. Before moving to 3D modelling that introduces challenges such as the requirement of high computational power, an analysis of the 2D model is carried out by solving most of the major physics involved in the process. The quantity of NOx production is computed at the post-processing stage. In the second subsection, a 3D non-reactive turbulent flow results are discussed. The flow results of the 3D model are compared with the 2D reactive flow model to show a necessity of 3D modelling especially while considering the mixing dominated rate of reaction in reactive flow modelling.

4.1. A 2D Reactive Flow Model of Heating Section of ABF

A 2D reactive flow model of the heating section of anode baking furnace is developed by gradually increasing the complexity of the model. At the first stage, modelling of a non-reactive turbulent flow model is carried out and validated by comparing with another simulation environment, IB-Raptor code [10]. These validated results provide a strong basis for the turbulent flow simulations as the flow is the most important physics in the process. Fig. 1 shows a comparison of two simulation

codes (COMSOL and IB Raptor code) with respect to velocity and viscosity ratio. It can be observed that the velocity magnitude and viscosity ratio generated by COMSOL Multiphysics software (Ref. code from Fig. 1) compares well with the IB Raptor code especially with the grid M (blue line). The comparison is elaborated well in the previous conference paper [10].

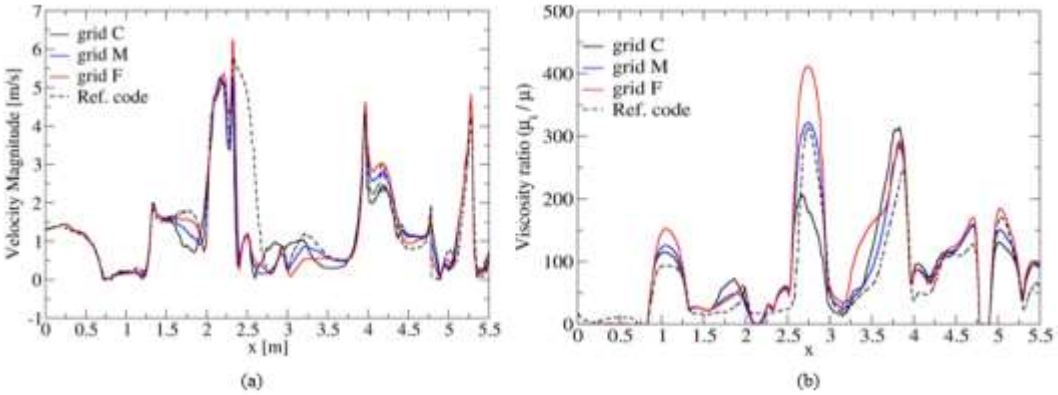

Fig. 1: Comparison of results of two simulation codes COMSOL (Ref. code) and IB Raptor code (grid C, M, F) (a) by comparing Velocity Magnitude and (b) Viscosity ratio on a horizontal line at a certain position in the 2D section of the furnace.

The surface plot of the velocity magnitude for the reactive flow model is as given in Fig. 2. These plots of velocity magnitude of 150 m/s and 200 m/s show a difference, especially near the fuel inlet. It can be observed that, for the jet velocity of 200 m/s, the velocity distribution in both horizontal and vertical direction is higher as compared to 150 m/s. This distribution later translates to the better distribution of temperature in the furnace. However, the available data from the actual furnace of Aluchemie, suggest that the currently used burner inject velocity at around 150 m/s. Therefore, further calculations are based on this injection velocity of fuel.

The eddy dissipation model described in section 2 enables computation of mass fractions of various species that are considered in the model. The mass fraction distribution is shown in Fig. 3 suggests that the mass fraction of CH_4 is highest near the fuel inlet and reacts as soon as it mixes with O_2. The boundary conditions of velocities and mass fraction of air and fuel are such that the mixture is a lean mixture, i.e., the oxidant is available in bulk. The mass fraction distribution of O_2 shows that there is still some oxygen left in the outlet stream (Appendix Fig. A1). The products, i.e., H_2O and CO_2 are formed in the reaction zone near both fuel inlets where CH_4 is mixed with O_2 and are distributed due to the flow. The mass fraction distribution of all species align with the velocity distribution shown in Fig. 2 and confirms that the transport is convection dominated.

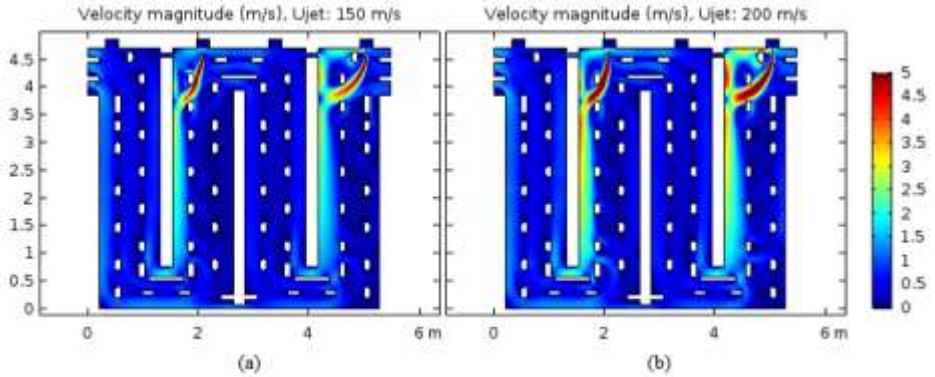

Fig. 2: Colour plots of velocity magnitude in 2D reactive turbulent flow model for fuel inlet velocity (Ujet) (a) 150 m/s and (b) 200 m/s. The range of legend is adjusted for better visualization of distribution of velocity magnitude. The maximum velocity in the furnace is higher than 5 m/s (153 m/s and 205 m/s, respectively).

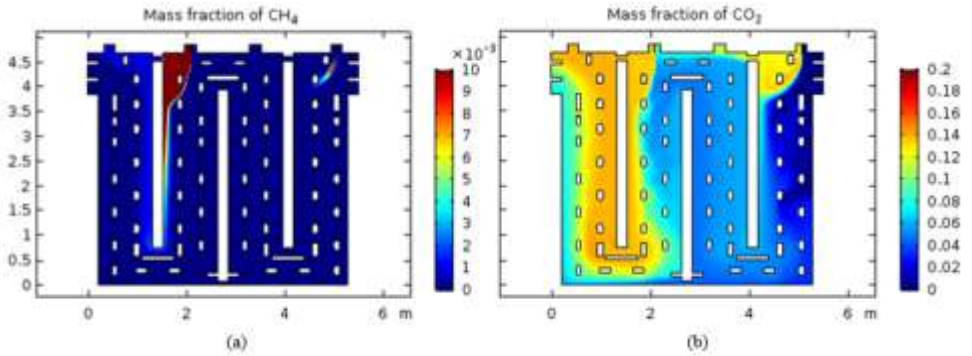

Fig. 3: Colour plots of mass fraction of species (a) CH_4 and (b) CO_2 in 2D reactive turbulent flow model. The range of legend is adjusted for better visualization of distribution of mass fraction. The maximum mass fraction in the furnace is different from the maximum legend (0.99 for CH_4, and 0.23 for CO_2).

The combustion reaction defined by eddy dissipation model releases heat which is a function of enthalpy of reaction. The numerical solution of the heat transport equation is as shown in Fig. 4 in terms of the parameters such as the temperature and heat of reaction released due to the combustion reaction. The reaction zone near the fuel inlet is prominent from the distribution of heat source. The temperature distribution from Fig. 4 shows that the majority of higher temperature zone is after the second fuel inlet when the complete combustion reaction in a section occurs. The maximum temperature observed by this model is 1770 K. It should be noted that this model does not yet consider the combustion of volatile matter. It is expected to have better distribution and higher temperature in the furnace by considering pitch combustion. Moreover, the eddy dissipation model is known for overpredicting the temperature due to lack of consideration of endothermic dissociation reaction of products. Therefore, the model needs further improvement before validating it with actual data. Nonetheless, this model provides good approximated surface distribution of parameters such as velocity, mass fractions and temperature that aligns with the expected physical nature.

As the high temperature is generated in the furnace, radiation significantly affects the temperature distribution. The product species, CO_2 and H_2O, are known as radiation absorbing species. The reactive turbulent flow model is extended by adding radiation with the P1 approximation model. The Planck mean absorption coefficient is defined by using 4^{th} order Gaussian function and corresponding fitting parameters [11]. The emissivity of refractory walls are defined as a function of temperature from the available experimental data. Fig. 5 shows the temperature distribution obtained as a result of radiation phenomena. The comparison of Fig. 4 (a) and Fig. 5 shows that the distribution of temperature is higher when the radiation is considered. It is expected that the radiation improves the transfer of heat thereby contributing to more uniform temperature distribution.

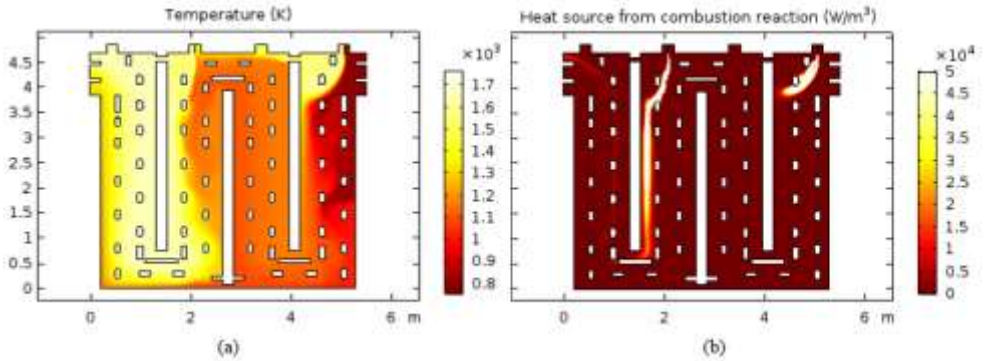

Fig. 4: Colour plots of (a) temperature and (b) heat source from combustion reaction in 2D reactive turbulent flow model (without radiation). The range of legend is adjusted for better visualization. The maximum temperature (1770 K) and heat released ($8*10^{10}$ W/m^3) are different from the legends.

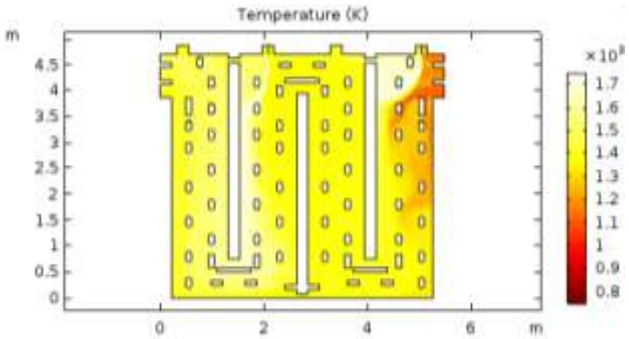

Fig. 5: Colour plot of temperature in the reactive turbulent flow model with radiation phenomena. The range of legend is adjusted for better visualization. The maximum temperature (1770 K) is different from the legends.

Further, in a post-processing stage, the distribution of NOx is computed based on the Zeldovich mechanism explained in Section 2. Fig. 6 shows that the NOx is formed in high-temperature regions. The mole fraction of NOx predicted by this model is very small as compared to the actual measured values. The difference is mainly due to the inaccurate prediction of temperature due to the reasons listed above. Furthermore, 2D modelling has their limitations mainly due to inconsistent mixing behaviour as compared to the reality. In the next subsection, results of non-reacting turbulent flow of the 3D model are presented. The comparison with the 2D shows the need for 3D models for better comparison with the actual data.

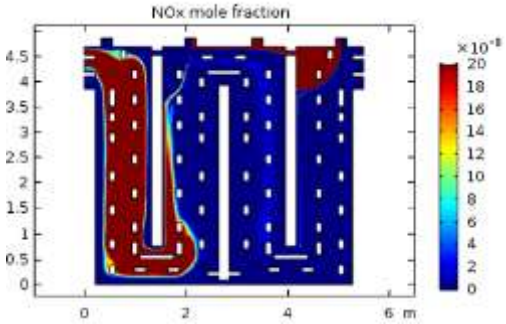

Fig. 6: Surface plot of distribution of mole fraction of NOx using Zeldovich mechanism.

4.2. Non-reactive turbulent flow modelling in 3D

Fig. 7 shows a velocity magnitude plot at the 2D center plane in XY direction. This 3D model has different boundary conditions as compared to the 2D model elaborated in section 4.1. For this 3D model, only one fuel inlet is considered. The air flow is from X coordinate 0 to X coordinate 5.5. The velocity magnitude at the center plane in XY direction shows a similarity of velocity distribution with a 2D model. However, a top view, i.e., the velocity distribution in XZ direction shows a significant difference.

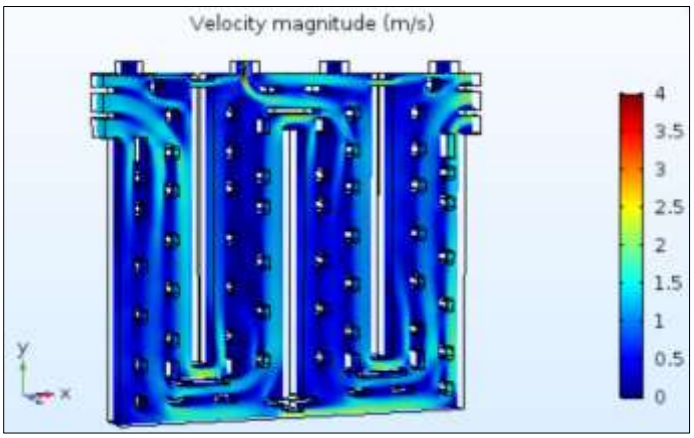

Fig. 6: Velocity magnitude at center plane in XY direction of the 3D non-reactive turbulent flow model. The range of legend is adjusted for better visualization. The maximum velocity in the furnace is higher than 4 m/s.

It can be seen from Fig. 7 that near the fuel inlet velocity distribution significantly varies in the Z direction. While, in a 2D model, the velocity in the Z direction is assumed to be constant. This difference needs a correction especially in reactive flow model in which the rate of reaction is mixing dominated.

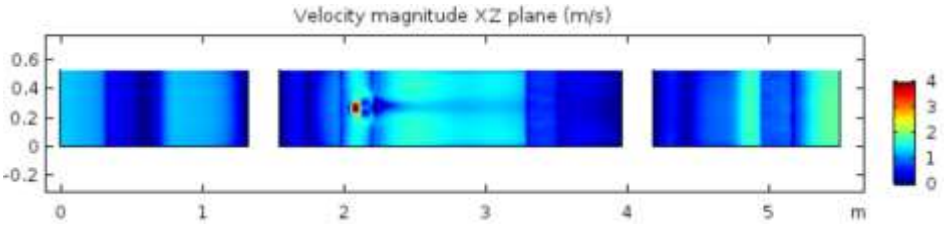

Fig. 7: Velocity magnitude in XZ direction of the 3D non-reactive turbulent flow mode.

5. Conclusion

In this work, COMSOL® Multiphysics software is used for modelling and it proves to provide results that align with expected physical behaviour. A 2D reactive turbulent flow model and 3D non-reactive flow model developed in this work deliver a validated flow field in the heating section of the anode baking process. It can be concluded that for mixing dominated combustion models such as the eddy dissipation model, a 3D model would be more accurate. However, computation of 2D reactive flow model is comparatively easier and can provide an understanding of the physical nature inside the furnace. In further work, a 2D model will be improved in terms of combustion and radiation modelling. The knowledge from the development of 2D reactive model would be used to develop a 3D reactive flow model with radiation.

Acknowledgements

We would like to thank Dr. Marco Talice from Pm2engineering, Cagliari, Italy for providing results with IB Raptor code for validation. We would also like to thank Aluminium & Chemie Rotterdam B.V. for their support.

References

[1] D. S. Severo and V. Gusberti, “User-friendly software for simulation of anode baking furnaces,” in *Proceeding of the 10th Australasian Aluminum Smelting Technology Conference*, 2011.

[2] N. Oumarou, D. Kocaefe, Y. Kocaefe, and B. Morais, “Transient process model of open anode baking furnace,” *Appl. Therm. Eng.*, vol. 107, pp. 1253–1260, 2016.

[3] Bui, R. T., Dernedde, E., Charette, A., and Bourgeois, T., "Mathematical simulation of a horizontal flue ring furnace." *Light Metals*. pp. 1033-1040, 1984.
[4] Y. S. Kocaefe, E. Dernedde, D. Kocaefe, R. Ouellet, Q. Jiao, and W. F. Crowell, "A 3D mathematical model for the horizontal anode baking furnace," *Light Met. Proc. Sess. TMS Annu. Meet. (Warrendale, Pennsylvania)*, pp. 529-534,1996.
[5] N. Oumarou, D. Kocaefe, and Y. Kocaefe, "An advanced dynamic process model for industrial horizontal anode baking furnace," *Appl. Math. Model.*, vol. 53, pp. 384–399, 2018.
[6] N. Oumarou, Y. Kocaefe, D. Kocaefe, B. Morais, and J. Lafrance, "A dynamic process model for predicting the performance of horizontal anode baking furnaces," in *Light Metals 2015*, Springer, pp. 1081–1086, 2015.
[7] F. Grégoire and L. Gosselin, "Comparison of three combustion models for simulating anode baking furnaces," *Int. J. Therm. Sci.*, vol. 129, pp. 532–544, 2018.
[8] A. R. Tajik, T. Shamim, R. K. A. Al-Rub, and M. Zaidani, "Two dimensional CFD simulations of a flue-wall in the anode baking furnace for aluminum production," *Energy Procedia*, vol. 105, pp. 5134–5139, 2017.
[9] A. R. Tajik, T. Shamim, M. Zaidani, and R. K. A. Al-Rub, "The effects of flue-wall design modifications on combustion and flow characteristics of an aluminum anode baking furnace-CFD modeling," *Appl. Energy*, vol. 230, pp. 207–219, 2018.
[10] P. Nakate, D.J.P Lahaye, C. Vuik and M. Talice, "Systematic development and mesh sensitivity analysis of a mathematical model for an anode baking furnace," in ASME 2018, 5TH Joint US-European Fluids Engineering Division Summer Meeting, Montreal, Canada, 2018.
[11] M. Chmielewski and M. Gieras, "Planck Mean Absorption Coecients of H2O, CO2, CO and NO for radiation numerical modeling in combusting flows," *J. Power Technol.*, vol. 95, no. 2, p. 97, 2015.

Appendix

Mass fraction of O_2 and H_2O are as shown in Fig. A1.

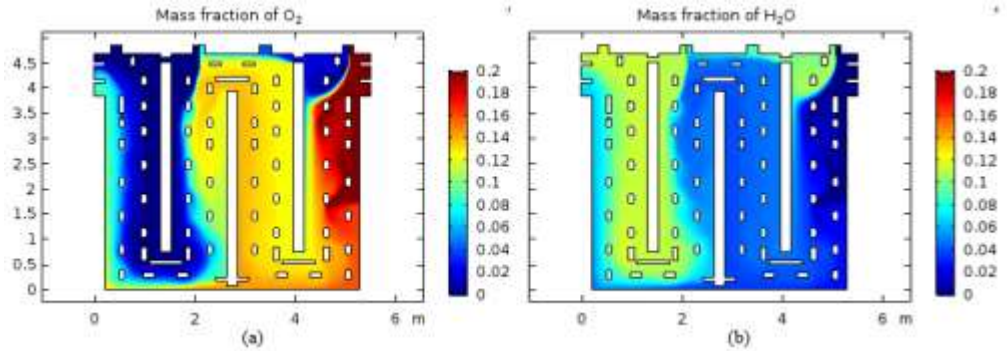

Fig. A1: Surface plots of mass fraction of species (a) O_2 and (b) H_2O in 2D reactive turbulent flow model. The range of legend is adjusted for better visualization of distribution of mass fraction. The maximum mass fraction in the furnace is different from the legend (0.23 for O_2, and 0.19 for H_2O).

List of Symbols

Symbol	Description	Symbol	Description
ρ	Density (Kg/m^3)	T	Temperature (K)
u	Velocity (m/s)	v_i	Stoichiometric coefficient of species i
p	Pressure (Pa)	M_i	Molecular weight of species i (Kg/mol)
μ	Dynamic viscosity (Pa*s)	α	Turbulent-reaction parameter
μ_T	Turbulent viscosity (Pa*s)	τ_T	Turbulent time scale (s)
k	Turbulent kinetic energy (m^2/s^2)	β	Turbulent-reaction parameter
σ_k	Turbulence parameter constant	d_z	Width is z direction (m)
σ_ε	Turbulence parameter constant	C_p	Specific heat capacity (J/Kg/K)
ε	Turbulent dissipation rate (m^2/s^3)	k	Thermal conductivity (W/m/K)
$C_{\varepsilon 1}$	Turbulence parameter constant	q_0	Heat source by combustion (W/m^3)
$C_{\varepsilon 2}$	Turbulence parameter constant	Q_r	Hear source by radiation (W/m^3)
C_μ	Turbulence parameter constant	κ	Absorption coefficient (1/m)
j_i	Diffusive flux of species i (Kg/m^{2}s)	G	Incident radiation (W/m^2)
w_i	Mass fraction of species i	I_b	Blackbody radiation (W/m^2/Sr)
R_i	Reaction rate of species i (Kg/m^{3}s)	σ_s	Scattering coefficient (1/m)
D_i^f	Ficks diffusion coefficient of species i (m^2/s)	S_{NO}	Source term of NO (1/s)
M_n	Mean molecular mass (Kg/mol)	$k_{r,1}k_{r,2}$	Reverse reaction coefficient of reaction 1 and 2
x_i	Mole fraction of species i	$k_{f,1}, k_{f,2}$	Forward reaction coefficient of reaction 1 and 2
D_i^T	Thermal diffusion coefficient (Kg/m/s)		